Transmitter IQ Imbalance Mitigation using 4×4 Real Value MIMO Equalizer Based on DD-LMS Algorithm

Zepeng Gong
China University of Geosciences
Wuhan 430074, China
gongzepeng@cug.edu.cn

Fan Shi
China University of Geosciences
Wuhan 430074, China
shifan@cug.edu.cn

Hanyong Wang
China University of Geosciences
Wuhan 430074, China
hanyong@cug.edu.cn

Yafeng Cheng
China University of Geosciences
Wuhan 430074, China
chengyf@cug.edu.cn

Tianye Huang
China University of Geosciences
Wuhan 430074, China
tianye_huang@163.com

Xiang Li
China University of Geosciences
Wuhan 430074, China
lix@cug.edu.cn

***Abstract*—We evaluated the performance of a 4×4 real value multiple-input-multiple-output (MIMO) equalizer with carrier phase recovery (CPR) based on the decision direct least mean square (DD-LMS) algorithm for transmitter IQ imbalance compensation. The effectiveness of the algorithm is verified by simulation based on 64-GBaud polarization multiplexing-16 quadrature amplitude modulation (PM-16QAM) formats. The results showed that the proposed method could achieve signal-to-noise ratio (SNR) penalties of only 0.35 dB, 0.37 dB, and 0.2 dB with 9 ps skew, 3 dB gain imbalance, and 10 degree phase error, respectively.**

Keywords—coherent optical communication, IQ imbalance, real value equalizer, digital signal processing

I. Introduction

Coherent optical communication techniques have been widely used due to their large capacity, high spectral efficiency, and the ability of transmission impairment mitigation through digital signal processing (DSP). Using high baud rate and high-order modulation is a straightforward way to handle the issue of traffic demand. Nevertheless, the implementation of a high-capacity transceiver suffers from problems including bandwidth limitation, device nonlinearity, and imbalances between in-phase (I) and quadrature (Q) tributaries [1].

To compensate for the IQ imbalances, several DSP algorithms, such as Gram-Schmidt orthogonalization procedure (GSOP) [2], 4×4 real-valued equalizer [3], and adaptive filtering algorithms [4, 5] at the coherent receiver have been proposed. However, the application of GSOP and 4×4 real-valued equalizer is limited to receiver (Rx) compensation and cannot be used for compensation of IQ imbalances on the transmitter (Tx) side. This is mainly because the equalization of the Tx side faces greater challenges for the receiver's DSP due to the presence of transmission impairments such as chromatic dispersion (CD), polarization mode dispersion (PMD), polarization rotation, and Rx device characteristics.

Several studies have been conducted to compensate for the IQ imbalances on the Tx side. One example is the blind adaptive source separation (BASS) method, which compensates for gain and phase imbalances [6]. However, integrating the BASS method into an equalizer requires more computation resources than the GSOP technique, as it involves additional addition and multiplication operators. Another approach is the clustering algorithm-based gain and phase imbalance estimation [7]. Additionally, the 2×2 real value (RV) multiple-input-multiple-output (MIMO) equalizer has been developed for imbalance compensation and calibration [8]. However, carrier phase recovery (CPR) has been individually performed prior to Tx impairment compensation in this case. This process may require large size fast Fourier transform (FFT), which significantly increases the computational complexity.

In this paper, we introduce a new method of mitigating IQ imbalance on the Tx side using a 4×4 RV MIMO equalizer with CPR based on the decision direct least mean square (DD-LMS) algorithm. Considering the phase sensitivity of the DD-LMS algorithm, fast phase fluctuations are removed from the error signal that adapts the FIR filter with long-delay taps, whereas phase estimation is done with only one-tap phase rotators. Based on this scheme, we are able to compensate for the phase noise, bandwidth limitation, polarization rotation, and IQ imbalance simultaneously.

The rest of the paper is organized as follows. The principle of the proposed algorithm is given in section II. In section III, we numerically evaluate its performance in the case of 64-GBaud polarization multiplexing-16 quadrature amplitude modulation (PM-16QAM). Results and the analysis of the impact of different impairments are displayed in section IV. Finally, we conclude our paper in section V.

II. 4×4 RV MIMO Equalizer with CPR in the Presence of IQ Imbalance

The conventional channel equalizer is depicted in Fig. 1. The in-phase and quadrature components of each polarization are combined into one complex input. This equalizer is a 2×2 MIMO with two complex inputs and two complex outputs. Considering it has only 4 complex-valued independent filters, the equalizer is not able to compensate for any imbalance between the in-phase and quadrature components [3].

The modified structure shown in Fig. 2 adds a 2×2 real value MIMO equalizer to each polarization, which separates in-phase and quadrature components for each polarization. During the channel equalization process, the complex signal

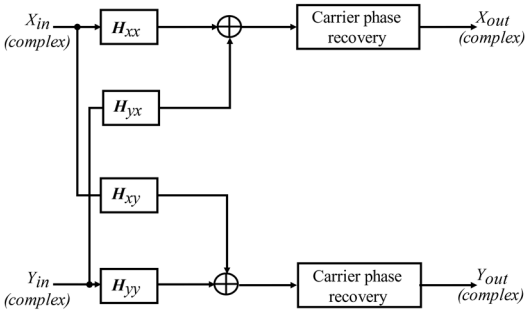

Fig. 1. Conventional 2×2 CV MIMO equalizer with CPR

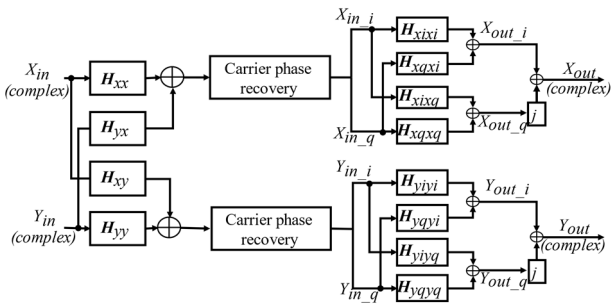

Fig. 2. Conventional 2×2 CV MIMO equalizer and 2×2 RV MIMO equalizer

X_{in} and Y_{in} are fed into the multiple-modulus algorithm (MMA) based 2×2 complex value (CV) MIMO equalizer for bandwidth limitation and polarization rotation compensation. Next, the carrier phase error is compensated by the CPR module in conjunction with frequency offset (FO) compensation for both polarizations. Finally, the 2×2 RV MIMO equalizer compensates for the Tx IQ imbalance for each polarization. The filter tap coefficients $\boldsymbol{H}_{xixi}$, $\boldsymbol{H}_{xqxi}$, $\boldsymbol{H}_{xixq}$, $\boldsymbol{H}_{xqxq}$, $\boldsymbol{H}_{yiyi}$, $\boldsymbol{H}_{yqyi}$, $\boldsymbol{H}_{yiyq}$ and $\boldsymbol{H}_{yqyq}$ are updated in the MMA algorithm.

The proposed 4×4 RV MIMO equalizer with CPR based on the DD-LMS algorithm is shown in Fig. 3. Differing from the 2×2 CV MIMO equalizer, it deploys 16 independent filters. Therefore, each of the four input components can have a different transfer function in the equalizer. These 16 independent filters receive input from both the real and imaginary components of the X and Y polarizations. Then, the output signals X_{out} and Y_{out} can be derived by combining the X_{out_i} and X_{out_q} signals and the Y_{out_i} and Y_{out_q} signals, respectively. By jointly updating the filters, the dual-stage decision-directed carrier-phase estimators can effectively eliminate the phase fluctuations caused by the laser phase noise and the frequency offset. Since the carrier phase is updated by using the complex signals after the 4×4 RV MIMO equalizer, the effectiveness of Tx IQ imbalance compensation is not affected by the carrier phase noise and frequency offset.

Let $X_{in\_i}(n)$ and $X_{in\_q}(n)$ respectively be the sampled real and imaginary parts of the X-polarization components. Similarly, let $Y_{in\_i}(n)$ and $Y_{in\_q}(n)$ be those for the Y-polarization components. Therefore, the column vector $\boldsymbol{X}_{in\_i}(n)$, $\boldsymbol{X}_{in\_q}(n)$, $\boldsymbol{Y}_{in\_i}(n)$ and $\boldsymbol{Y}_{in\_q}(n)$ can be given by

$$\boldsymbol{X}_{in\_i}(n) = [X_{in\_i}(n), X_{in\_i}(n-1),..., X_{in\_i}(n-M)]^T \quad (1)$$

$$\boldsymbol{X}_{in\_q}(n) = [X_{in\_q}(n), X_{in\_q}(n-1),..., X_{in\_q}(n-M)]^T$$

$$\boldsymbol{Y}_{in\_i}(n) = [Y_{in\_i}(n), Y_{in\_i}(n-1),..., Y_{in\_i}(n-M)]^T$$

$$\boldsymbol{Y}_{in\_q}(n) = [Y_{in\_q}(n), Y_{in\_q}(n-1),..., Y_{in\_q}(n-M)]^T$$

where M is the filter order and T stands for the transpose of a matrix.

The delay-tap coefficient vector $\boldsymbol{H}_{xixi}$, $\boldsymbol{H}_{xqxi}$, $\boldsymbol{H}_{yixi}$, $\boldsymbol{H}_{yqxi}$, $\boldsymbol{H}_{xixq}$, $\boldsymbol{H}_{xqxq}$, $\boldsymbol{H}_{yixq}$, $\boldsymbol{H}_{yqxq}$, $\boldsymbol{H}_{xiyi}$, $\boldsymbol{H}_{xqyi}$, $\boldsymbol{H}_{yiyi}$, $\boldsymbol{H}_{yqyi}$, $\boldsymbol{H}_{xiyq}$, $\boldsymbol{H}_{xqyq}$, $\boldsymbol{H}_{yiyq}$, $\boldsymbol{H}_{yqyq}$ can be given in a similar way. Each tap vector is updated as

$$\boldsymbol{H}_{xixi}(n+1)=\boldsymbol{H}_{xixi}(n)+\mu e_{xi}(n)\boldsymbol{X}_{in\_i}(n)^* \quad (2)$$

$$\boldsymbol{H}_{xqxi}(n+1)=\boldsymbol{H}_{xqxi}(n)+\mu e_{xi}(n)\boldsymbol{X}_{in\_q}(n)^*$$

$$\boldsymbol{H}_{yixi}(n+1)=\boldsymbol{H}_{yixi}(n)+\mu e_{xi}(n)\boldsymbol{Y}_{in\_i}(n)^*$$

$$\boldsymbol{H}_{yqxi}(n+1)=\boldsymbol{H}_{yqxi}(n)+\mu e_{xi}(n)\boldsymbol{Y}_{in\_q}(n)^*$$

$$\boldsymbol{H}_{xixq}(n+1)=\boldsymbol{H}_{xixq}(n)+\mu e_{xq}(n)\boldsymbol{X}_{in\_i}(n)^*$$

$$\boldsymbol{H}_{xqxq}(n+1)=\boldsymbol{H}_{xqxq}(n)+\mu e_{xq}(n)\boldsymbol{X}_{in\_q}(n)^*$$

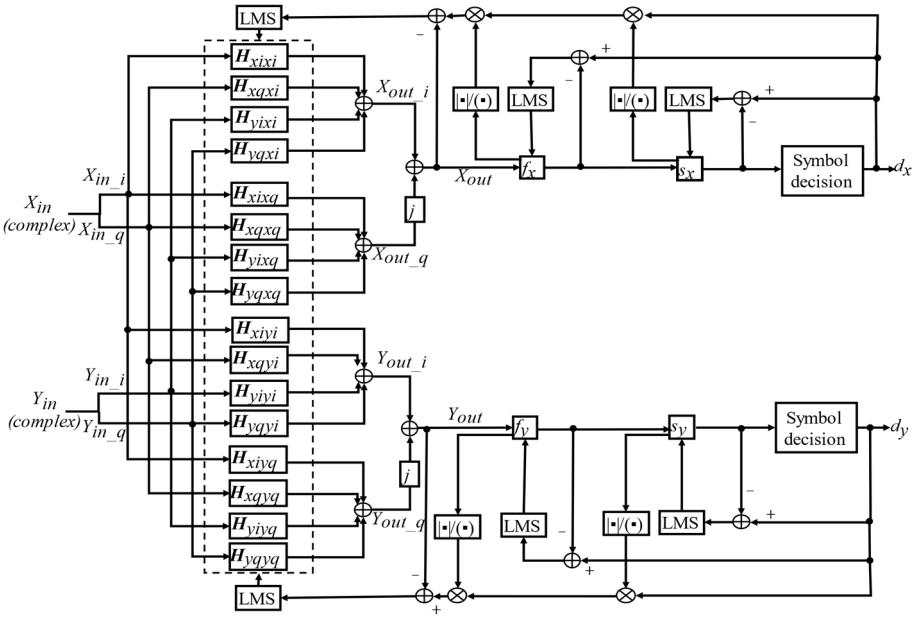

Fig. 3. Proposed 4×4 RV MIMO equalizer with CPR

$$\boldsymbol{H}_{yixq}(n+1)=\boldsymbol{H}_{yixq}(n)+\mu e_{xq}(n)\boldsymbol{Y}_{in\_i}(n)^*$$
$$\boldsymbol{H}_{yqxq}(n+1)=\boldsymbol{H}_{yqxq}(n)+\mu e_{xq}(n)\boldsymbol{Y}_{in\_q}(n)^*$$

$$\boldsymbol{H}_{xiyi}(n+1)=\boldsymbol{H}_{xiyi}(n)+\mu e_{yi}(n)\boldsymbol{X}_{in\_i}(n)^*$$
$$\boldsymbol{H}_{xqyi}(n+1)=\boldsymbol{H}_{xqyi}(n)+\mu e_{yi}(n)\boldsymbol{X}_{in\_q}(n)^*$$
$$\boldsymbol{H}_{yiyi}(n+1)=\boldsymbol{H}_{yiyi}(n)+\mu e_{yi}(n)\boldsymbol{Y}_{in\_i}(n)^*$$
$$\boldsymbol{H}_{yqyi}(n+1)=\boldsymbol{H}_{yqyi}(n)+\mu e_{yi}(n)\boldsymbol{Y}_{in\_q}(n)^*$$

$$\boldsymbol{H}_{xiyq}(n+1)=\boldsymbol{H}_{xiyq}(n)+\mu e_{yq}(n)\boldsymbol{X}_{in\_i}(n)^*$$
$$\boldsymbol{H}_{xqyq}(n+1)=\boldsymbol{H}_{xqyq}(n)+\mu e_{yq}(n)\boldsymbol{X}_{in\_q}(n)^*$$
$$\boldsymbol{H}_{yiyq}(n+1)=\boldsymbol{H}_{yiyq}(n)+\mu e_{yq}(n)\boldsymbol{Y}_{in\_i}(n)^*$$
$$\boldsymbol{H}_{yqyq}(n+1)=\boldsymbol{H}_{yqyq}(n)+\mu e_{yq}(n)\boldsymbol{Y}_{in\_q}(n)^*$$

where μ is the step-size parameter, the superscript * denotes complex conjugation, and $e_{xi,yi}(n)$ and $e_{xq,yq}(n)$are the real and imaginary parts of $e_{x,y}(n)$, respectively. The error signal $e_x(n)$, $e_y(n)$ are expressed as

$$e_x(n)=d_x(n)\{f_x(n)/|f_x(n)|\}^{-1}\{s_x(n)/|s_x(n)|\}^{-1}-X_{out}(n) \quad (3)$$
$$e_y(n)=d_y(n)\{f_y(n)/|f_y(n)|\}^{-1}\{s_y(n)/|s_y(n)|\}^{-1}-Y_{out}(n)$$

where $d_{x,y}(n)$ denotes either the desired signal in the training mode or the decoded signal in the tracking mode. The first-stage and second-stage phase estimators estimate the complex numbers $f_{x,y}(n)$ and $s_{x,y}(n)$, respectively.

The output of the 4×4 RV MIMO equalizer is then calculated as

$$X_{out}(n) = X_{out\_i}(n) + jX_{out\_q}(n) \quad (4)$$
$$Y_{out}(n) = Y_{out\_i}(n) + jY_{out\_q}(n)$$

As for the dual-stage phase estimators, the tap coefficient of the first-stage phase estimator $f_{x,y}(n)$ is updated as

$$f_{x,y}(n+1)=f_{x,y}(n)+\frac{\mu_f}{|V_{x,y}(n)|^2+\varepsilon}e_{fx,y}(n)V_{x,y}(n)^* \quad (5)$$

$$e_{fx,y}(n)=d_{x,y}(n)-f_{x,y}(n)V_{x,y}(n)$$

where μ_f is the step-size parameter, $e_{fx,y}(n)$ is the error signal controlling the tap coefficient of the first-stage phase estimator, ε is the small positive offset, and $V_{x,y}(n)$ denotes the output signal of the MIMO equalizer, $X_{out}(n)$ or $Y_{out}(n)$. On the contrary, the tap coefficient of the second phase estimator $s_{x,y}(n)$ is updated by

$$s_{x,y}(n+1)=s_{x,y}(n)+\frac{\mu_s}{|f_{x,y}(n)V_{x,y}(n)|^2+\varepsilon}e_{sx,y}(n)\{f_{x,y}(n)V_{x,y}(n)\}^* \quad (6)$$

$$e_{sx,y}(n)=d_{x,y}(n)-s_{x,y}(n)f_{x,y}(n)V_{x,y}(n)$$

where μ_s is the step-size parameter. The tap coefficient of the second-stage phase estimator is controlled by the error signal $e_{sx,y}(n)$.

III. Simulation Setup

We conducted a numerical simulation to evaluate the effectiveness of the 4×4 RV MIMO equalizer with CPR for dual polarization transmission employing 16-QAM modulation format. The numerical simulation model is depicted in Fig. 4. For all simulation scenarios, we assumed a symbol rate of 64-GBaud. In the constellation mapping block, the sequences of 16-QAM symbols were generated with a predetermined length of 16384 symbols per polarization, mapped from decorrelated segments of pseudo-random bit sequences (PRBS). The modulated data was upsampled to 8 samples per symbol, and pulse shaped using root raised cosine (RRC) filters with the roll-off factor of 0.1. The Tx IQ skew, Tx IQ gain imbalance were digitally emulated for X polarization, and quadrature phase was manually shifted for X polarization to generate the skew. For all tested cases, phase noise was set to 100 kHz. A fixed frequency offset of 100 MHz was assumed between the local oscillators at transmitter and receiver in most simulations, except for an additional simulation without frequency offset for comparison in the scheme shown in Fig. 2.

The simplified linear optical channel model used accounted for static linear polarization rotation, and amplified spontaneous emission (ASE) from Erbium doped fiber amplifiers (EDFAs), modeled as additive white Gaussian noise (AWGN) loading stage.

At the receiver side, the received signal was pulse deshaped using RRC filters with the roll-off factor of 0.1, and aligned with the half symbol duration through downsampling. This stage is followed by a standard set of DSP algorithms, as shown in Fig. 4. Here， three MIMO configurations were evaluated: (1) T/2-spaced 2×2 CV MIMO equalizer, which we described in Fig. 1, (2) T/2-spaced 2×2 CV MIMO equalizer with T-spaced 2×2 RV MIMO after CPR, shown in Fig. 2, and (3) the proposed 4×4 RV MIMO, as shown in Fig. 3. Note that, 2×2 CV MIMO equalizer only was applied for the benchmark of Tx IQ imbalance. For the proposed scheme, as described in the previous section, the filter coefficient was updated with DD-LMS algorithm, which was different from the MMA algorithm used in the 2×2 CV MIMO equalizer. After demodulating the signals, we calculated the effective signal-to-noise ratio (SNR) for comparison among the three algorithms. The filters had 33 taps for T/2-spaced MIMO and 5 taps for T-spaced MIMO.

IV. Results and Discussion

We evaluated the performance of the 4×4 RV MIMO equalizer for 64-GBaud PM-16QAM transmission, using the 2×2 CV MIMO equalizer as a baseline. The effective SNR is used to evaluate the system's performance.

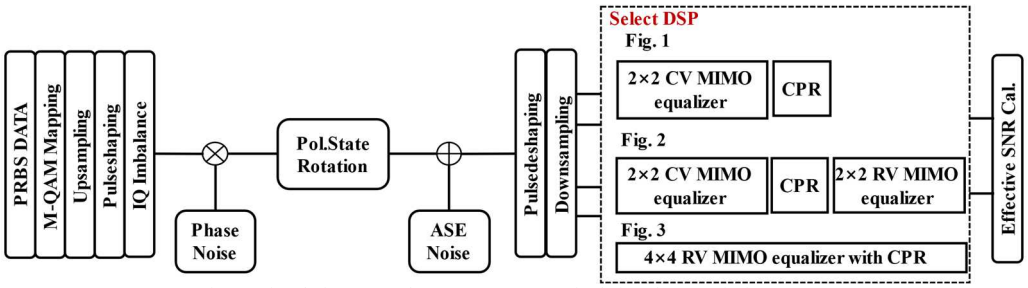

Fig. 4. Simulation setup for PM-16QAM optical signal transmission system

Fig.5 shows the effective SNR as a function of IQ skew, where only the effective SNR of the X polarization is considered. The 4×4 RV MIMO equalizer outperformed the other equalizers, while the 2×2 CV MIMO equalizer suffered from IQ skew imbalance resulting in a large degradation of effective SNR. The 2×2 RV MIMO equalizer can mitigate the impairment of IQ skew to some extent. It can be seen that the 2×2 RV MIMO equalizer resulted in a degradation of more than 8 dB at the IQ skew of 4 ps. It is also noted that the performance of the 2×2 RV MIMO equalizer degraded seriously in the presence of frequency offset, which is the same as that of the 2×2 CV MIMO equalizer. As shown in Fig. 5, The proposed method only suffers from the penalty of 0.35 dB at 9 ps, which shows much higher tolerance than conventional methods.

Fig. 6 shows the effective SNR as a function of IQ gain imbalance for X polarization. Similar to Fig. 5, the 4×4 RV MIMO equalizer demonstrated the best performance. For a 3 dB gain imbalance, the 2×2 RV MIMO equalizer resulted in a penalty of 7.3 dB, while the proposed method only showed a penalty of 0.37 dB. Again, it is observed that the 2×2 RV MIMO equalizer cannot compensate for the IQ gain imbalance if frequency offset exists.

Fig. 7 illustrates the impact of the quadrature phase error of the X polarization on the effective SNR performance. The 2×2 CV MIMO equalizer's performance gradually degraded with increasing phase error, whereas for the 4×4 RV MIMO equalizer, only small effective SNR penalties up to 7 degrees were observed, and a penalty of 0.2 dB is obtained at 10 degrees. The 2×2 RV MIMO equalizer can also compensate for the phase error if frequency offset is not considered. The penalty is 2.4 dB if the phase error is 10 degrees.

The simulation results in Fig. 5 to Fig. 7 suggest that the proposed method is more robust to Tx IQ imbalance, which can effectively mitigate the impairments of IQ imbalance from the transmitter side.

V. Conclusion

We have proposed a 4×4 RV MIMO equalizer with CPR based on the DD-LMS algorithm for Tx IQ imbalance compensation. It can simultaneously compensate the polarization rotation, Tx IQ imbalance, and carrier phase noise with dual-stage phase estimators.

In the simulation for 64-GBaud PM-16QAM transmission with Tx IQ skew, Tx IQ gain imbalance, and quadrature error in X polarization, the proposed method is compared with the conventional 2×2 RV MIMO equalizer. Our results demonstrated that our proposed method can provide superior performance than other methods, with only effective SNR penalties of 0.35 dB at skew of 9 ps, 0.37 dB at gain imbalance of 3 dB, and 0.2 dB at phase error of 10 degree, respectively.

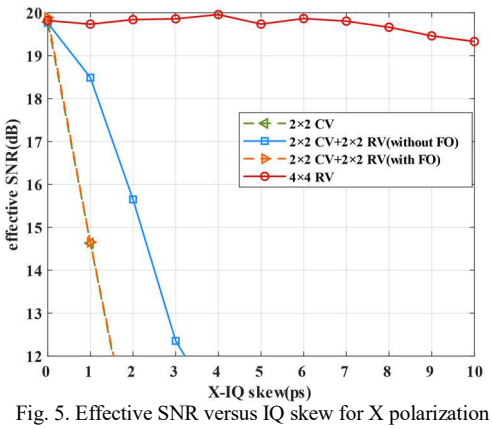

Fig. 5. Effective SNR versus IQ skew for X polarization

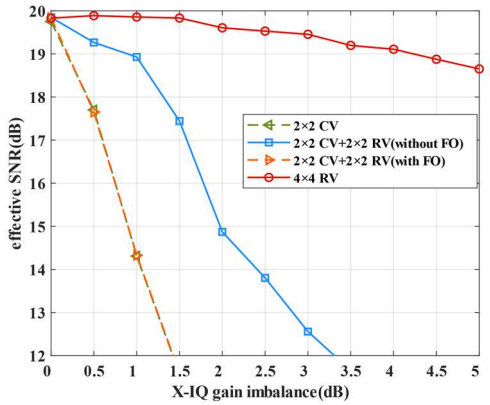

Fig. 6. Effective SNR versus IQ gain imbalance for X polarization

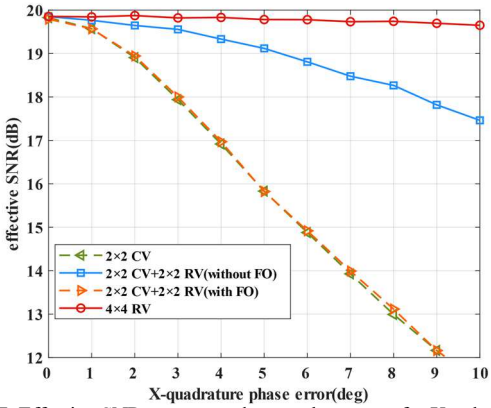

Fig. 7. Effective SNR versus quadrature phase error for X polarization

References

[1] Y. Fan et al., "Experimental verification of IQ imbalance monitor for high-order modulated transceivers," in 2018 European Conference on Optical Communication (ECOC), 2018, pp. 1–3.

[2] I. Fatadin, S. J. Savory, and D. Ives, "Compensation of quadrature imbalance in an optical QPSK coherent receiver," IEEE Photonics Technology Letters, vol. 20, no. 20, pp. 1733–1735, 2008.

[3] M. Paskov, D. Lavery, and S. J. Savory, "Blind equalization of receiver in-phase/quadrature skew in the presence of Nyquist filtering," IEEE Photonics Technology Letters, vol. 25, no. 24, pp. 2446–2449, 2013.

[4] T. Kobayashi et al., "35-Tb/s C-band transmission over 800 km employing 1-Tb/s PS-64QAM signals enhanced by complex 8×2 MIMO equalizer," in 2019 Optical Fiber Communications Conference and Exhibition (OFC), 2019, pp. 1–3.

[5] E. P. da Silva and D. Zibar, "Widely linear equalization for IQ imbalance and skew compensation in optical coherent receivers," Journal of Lightwave Technology, vol. 34, no. 15, pp. 3577–3586, 2016.

[6] T.-H. Nguyen et al., "Blind transmitter IQ imbalance compensation in M-QAM optical coherent systems," Journal of optical communications and networking, vol. 9, no. 9, pp. D42–D50, 2017.

[7] Q. Zhang et al., "Algorithms for blind separation and estimation of transmitter and receiver IQ imbalances," Journal of Lightwave Technology, vol. 37, no. 10, pp. 2201–2208, 2019.

[8] C. R. Fludger and T. Kupfer, "Transmitter impairment mitigation and monitoring for high baud-rate, high order modulation systems," in ECOC 2016; 42nd European Conference on Optical Communication, 2016, pp. 1–3.